End-of-century heat and drought stress approaching Europe swiftly

Laura Suarez-Gutierrez (laura.suarez@mpimet.mpg.de)
ETH Zurich https://orcid.org/0000-0002-0008-5943
Wolfgang Müller
Max Planck Institute for Meteorology
Jochem Marotzke
Max Planck Institute for Meteorology https://orcid.org/0000-0001-9857-9900

Article

Keywords:

Posted Date: April 7th, 2023

DOI: https://doi.org/10.21203/rs.3.rs-2688096/v1

Additional Declarations: There is **NO** Competing Interest.

End-of-century heat and drought stress approaching Europe swiftly

Laura Suarez-Gutierrez[1,2,3,*], Wolfgang A. Müller[1], and Jochem Marotzke[1]

1. Max Planck Institute for Meteorology, Hamburg, Germany
2. Institute for Atmospheric and Climate Science, ETH Zurich, Zurich, Switzerland
3. Institut Pierre-Simon Laplace, CNRS, Paris, France

*Corresponding author: laura.suarez@mpimet.mpg.de

Abstract

Extreme heat and drought levels typical of an end-of-century climate could occur swiftly, and repeatedly. Despite the European climate being potentially prone to multi-year successive extremes due to the influence of the North Atlantic variability, it remains unclear how the likelihood of such successive extremes changes under warming, how early they could reach end-of-century levels, and how this is affected by internal climate variability. Using the MPI Grand Ensemble, we find that even under moderate warming, end-of-century heat and drought levels virtually impossible 20 years ago reach 1-in-10 likelihoods as early as the 2030s. By 2050-2075, two successive years of single or compound end-of-century extremes, unprecedented to date, exceed 1-in-10 likelihoods; while Europe-wide 5-year megadroughts become plausible. Whole decades of end-of-century heat stress could start by 2040, by 2020 for rain-deficit drought, and end-of-century decades starting as early as 2030 become twice as likely under a warm North Atlantic state.

Main

Under further global warming, extreme heat will become more likely, and more extreme[1]. However, currently extremely rare 'end-of-century' events — those that would be average in a much warmer world at the end of the century — can happen earlier than expected due to internal variability. In Europe, this occurred during the 2010 summer, which reached heat levels expected every other year by the end of the century[2]; but at the time it happened was deemed extremely rare[3], remaining the warmest summer observed over most of Europe. Record-shattering extreme heat events that exceed previous records by large amounts will become up to seven times more likely in the next three decades than they were in the recent past[4]. However, we still lack a systematic understanding of how soon typical end-of-century levels of extreme heat and drought stress become a possibility over Europe.

Extreme heat, especially at levels going substantially beyond our previous adaptability range, leads to increased heat-related mortality and morbidity[5]. In the last 30 years, up to 30% of heat-related deaths globally can be attributed to anthropogenic climate change[6]. In addition to the loss of human lives, extreme heat can lead to substantial ecological and socio-economic impacts, such as decreased labor productivity[7], increased risks of economic losses[8], wildfires[9], crop loss[10], and may even render some regions partially uninhabitable[11]. These far-reaching impacts are exacerbated when maximum temperatures compound with other system stressors[12], such as high humidity[11], lack of nighttime cooling[13], or persistent drought[14]. Extreme heat and humidity and insufficient infrastructure caused the death of thousands in the 2015 heatwaves in India and Pakistan[15]. In Europe, extreme heat and lack of nighttime cooling brought more than 70.000 additional deaths during the 2003 summer[16]. In 2018, the persistent drought and extreme temperatures over Central Europe triggered massive forest mortality events of unprecedented scale[17] and a 50% reduction in agricultural yields[18]. The impacts of extreme drought stress are further amplified under an increased volatility between severely dry and wet conditions; which hinders successful water management and accentuates the risk of wildfires, flooding, and mudslides[19].

Furthermore, when these extreme conditions occur repeatedly year after year, they become even more threatening to the already vulnerable socioeconomic and ecological resilience of the region[12,20,21,22]. Europe could be especially prone to such year-after-year successive heat and drought extremes, due to the influence of the multi-year variability in the North Atlantic over the European climate[23,24,25,26,27,28,29] acting as a long-term preconditioner. Despite the relevance of their potential cascading impacts and preconditioning in the European climate, it remains unclear how the likelihood of such multi-year successions of extreme heat and drought changes under warming, and moreover, how this likelihood is affected by the internal variability of the climate system.

The intensification of heat and drought, either independently or together, is attributed to be largely anthropogenic and is expected to be accentuated over Europe under further warming[30,31,32,33,34]. However, changes in the frequency and intensity of heat and drought stress depend not only on the level of global warming; they can also be dampened or amplified by internal variability on interannual to multi-decadal scales[2,26,33]. For example, the slowly evolving variability in the North Atlantic system affects European temperatures in observations[35,36,37], and modulates past observed trends in concurrent heat and drought over European croplands[26]. This linkage has been also identified in idealized numerical experiments imposing slowly evolving sea surface temperature (SST) patterns to emulate different phases of Atlantic Multidecadal Variability (AMV), which lead to a marked increase in temperature and slightly lower decrease in precipitation under positive versus negative AMV phases[27,28]. The mechanism behind this link involves barotropic wave-train structures driven by the warm North Atlantic states, which in particular for Europe implies dry anticyclonic conditions concurring with near-surface warm-air advection and adiabatic heating[35,38].

These oceanic origins of concurrent atmospheric drivers of heat and drought imply a long-term preconditioning on decadal timescales that may make the European climate system particularly prone to such year-after-year successive high-impact heat and drought stress extremes. Moreover, while extreme temperature and precipitation predictions over Europe for the next few months to years remain substantially uncertain; the AMV is thought to be one of the most predictable aspects of decadal climate[39]. Therefore, improving our understanding of how the relatively predictable AMV affects successive and compounding heat and drought stress is crucial for both the prediction and the attribution of such low-probability, high-impact events. In turn, more robust prediction and attribution of such events would greatly improve our preparedness and the efficiency of our adaptation and mitigation efforts.

We provide the first systematic assessment of how soon different forms of end-of-century heat and drought stress could occur over Europe, and the role that the decadal variability in the North Atlantic plays in this outcome, with a twofold impact-relevant focus. This impact-relevant perspective comes, first, from assessing the likelihood of successive, year-after-year extremes; and second, from focusing both on single and compound heat and drought metrics reflecting potential compounding and cascading hazards. Our ultimate goal is to determine how internal climate variability leads to worst-case successive and compounding heat and drought stress accumulating to produce the most extreme decades, and how soon into the near future such heat and drought loaded decades could bring a taste of the end-of-the-century reality.

For this we use excess metrics that combine the effects of both intensity and persistency of all events within a season[40], as a sum of every instance beyond a given threshold (see Methods). We expand the existing Excess Heat framework[40] based on maximum temperatures to cover three additional novel excess metrics that reflect extreme heat and drought stress: Humid Heat, Night Heat, and Rain Deficit. In addition to these four types of single heat and drought stress extremes, we also assess three compound heat and drought stress types: Compound Heat Stress, Compound Heat and Drought, and Drought-Rain Volatility. For this we use the 100-member Max Planck Institute Grand Ensemble[41], under historical and RCP4.5 forcing leading to roughly 2.25C of warming by the end of the century[2].

MPI-GE is the largest existing initial-condition ensemble of a comprehensive, fully coupled Earth System Model currently available. This large ensemble size is crucial for robustly sampling and assessing changes in low-probability univariate events, and it is even more important for multivariate compound events and temporally successive extremes[42]. In addition to its large ensemble size, compared to other large ensembles MPI-GE also offers one of the most adequate representations of the historical internal variability and forced changes in observed temperatures[43] and precipitation[44]. For these reasons, MPI-GE is the best-available tool for this first assessment of how soon internal climate variability could bring end-of-century levels of successive extreme heat and drought stress upon Europe.

Excess Heat and Drought Projections

By the end of the 21^{st} century and even under moderate warming, extreme heat and drought stress will increase intensely over Europe, with practically all simulated years exhibiting levels well beyond recent-past average conditions as early as 2040 (Fig. 1). However, and even more importantly, worst-case years at the upper tails of the distributions show an even more marked increase than the average, with deviations from their concurrent average climate of unprecedented scale. For all heat metrics, typical end-of-century extremes, defined as the 2090-2099 average, become plausible albeit rare already in 2000-2009. MPI-GE simulates summers as extreme as the 2010 record already 5 to 10 years prior. These end-of-century summers, virtually impossible only 20 years ago and a rare occurrence in the last decades, reach 1-in-10 chances already in 2030-2039 for all heat metrics.

For a typical end-of-century summer, Excess Heat reaches values almost 10 times as high as the 1950-1999 average, while extreme end-of-century summers at the upper tail of the distribution (beyond 90^{th} percentile) reach values 20 to 35 times as high, with similar tendencies for Night Heat. For Humid Heat, this increase is less marked and the upper tail summers reach levels 10-15 times higher than the 1950-1999 average, with somewhat smaller differences between average and higher-percentile summers. For excess Rain Deficit, the distribution is centered around values roughly twice as large than the recent past average by the end of the century. The most extremely dry years reach rain deficits 3 to 8 times higher than the 1950-1999 average. Thus, all forms of extreme heat become more prevalent and intense by the end of the century than in the recent past; while rain deficits below current-climate thresholds suffer a less substantial increase in comparison in MPI-GE.

These projections are based on an adequate representation of the magnitude, variability and forced changes under warming in E-OBS observations by MPI-GE for all excess metrics in the period of 1950-2021 (SI Fig. S1). Our evaluation shows that E-OBS observations are mostly within the ensemble spread and well within the perfect model range of MPI-GE (further details on this evaluation framework described in ref.[43]). Furthermore, also the frequency of heat and drought extremes is well captured by MPI-GE, with good agreement between simulated and observed number of days (months for Rain Deficit) above threshold per year (not shown). In the observed period, 2010 stands out as the summer exhibiting the most extreme heat over Europe. It reached heat levels 10 times higher than the 1950-1999 average across all metrics, and roughly coincides with the 1-in-100-members ensemble maxima for the concurrent period. For Rain Deficit, 2015 stands out as the year with the most extreme lack of precipitation, roughly coinciding with the 90^{th} percentile of the ensemble distribution. However, none of the observed rain deficits are quite as extreme as concurrent MPI-GE ensemble maxima, indicating that MPI-GE may overestimate the risk and magnitude of rain-deficit drought, or that an event as rare on a continental-scale has not yet occurred.

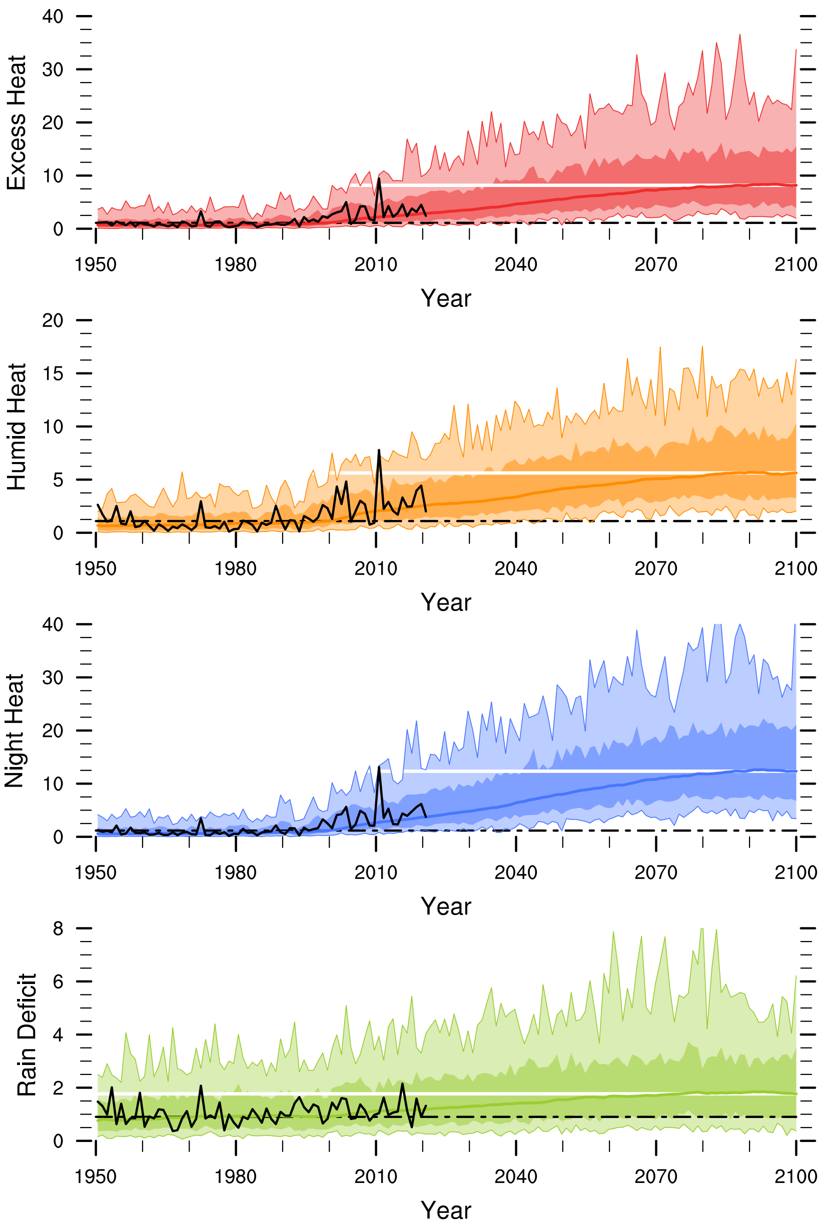

Figure 1: **Excess Metrics for MPI-GE against E-OBS.** Time series of Summer (JJA) Excess Heat (red), Humid Heat (orange), Night Heat (blue), and May-October Rain Deficit (green; see methods for metric definitions) simulated by MPI-GE (color) against E-OBS observations (black; 1950-2021). Light shading represents the full ensemble spread; dark shading represents the 10th-90th percentile range of the ensemble. Thick colored lines show the 10-year average of the 50th percentile of the ensemble. The black dashed line represents this 50th percentile at the end of the 20th century, averaged over the period of 1990-1999; while the white line represents this 50th percentile the end of the 21st century, averaged over 2090-2099. Each metric is shown as a ratio with respect to its average over the period of 1950-1999, and is averaged over the European region defined by the [35–63N, 10W–55E] domain. MPI-GE simulations are historical (1950-2005) and RCP4.5 (2006-2099) and subsampled to land grid cells where observations are available.

Typical end-of-century extreme heat has a less than 5% chance of occurring during any single year in the 2000-2024 period (Fig. 2). In the next 25 years this likelihood increases to 10-15%, meaning that one or more summers in every 10 could exceed end-of-century levels. By 2050-2075, this likelihood rises to more than a third. Moreover, the likelihood that after one of such end-of-century extreme summers we experience another one goes from virtually zero to 2-4% in the next 25 years. By 2050-2075, the likelihood of two successive summers of end-of-century heat exceeds 15%, with up to a 3% chance of year-after-year end-of-century extreme heat occurring for 5 consecutive years. On the other hand, the likelihood of end-of-century rain deficit drought stress stands at 20% during recent decades, and rises to over 30% in the next 25 years. The likelihood of two consecutive years of end-of-century drought stress caused by an extreme lack of rain almost triples in the next 25 years compared to the recent past to almost 15%. Lastly, with likelihoods over 3,5% by 2050-2075, unprecedent 5-year long mega-droughts affecting the whole European continent, although rare, become plausible.

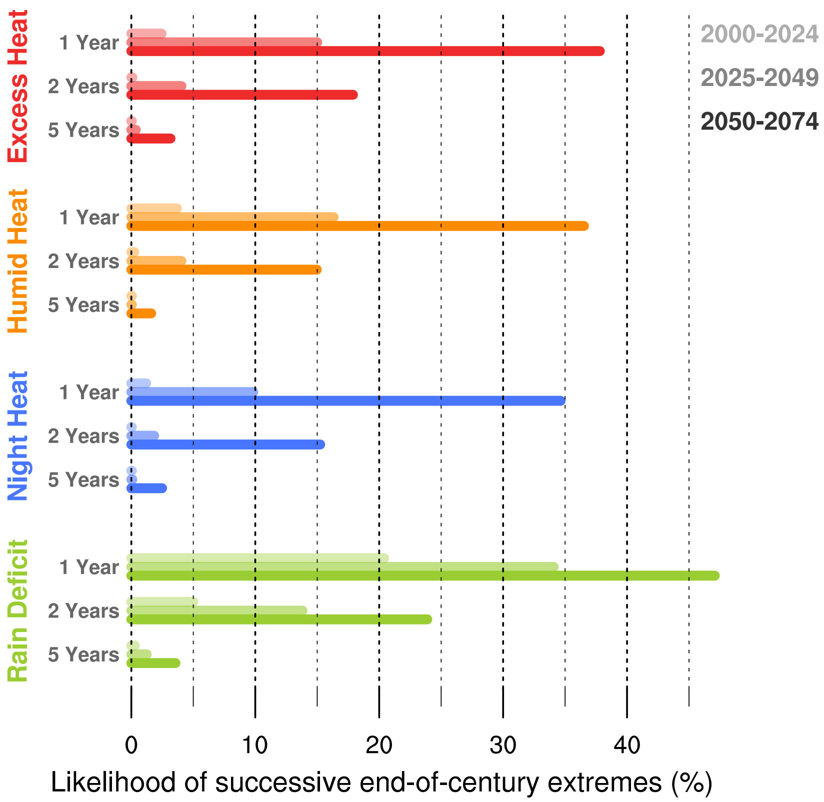

Figure 2: **Likelihood of successive end-of-century extremes.** Likelihood of extremes occurring in one year, and that the following 2 or 5 years, also exhibit extreme excess metrics, for the periods of starting in the years 2000-2024 (light colors), 2025-2049 (medium colors) and 2050-2074 (dark colors). Extreme years are defined as those equal or larger than the end-of-century 50th ensemble percentile averaged over the period of 2090-2099.

The likelihood of end-of-century extremes compounding in any given year also becomes substantially higher in the next decades (Fig. 3). A single year of end-of-century Compound Heat Stress or Compound Heat and Drought, both extremely rare combinations in the recent past, could occur during one out of every 10 summers in the next 25 years, and roughly 1 out of every 3 by 2050. The likelihood of experiencing successive end-of-century compound extremes for two consecutive years, virtually zero in the recent past, rises to over 1-in-10 in the 2050-2075 period. And while compound year-after-year extremes for 5 consecutive summers remain rare, they could by then become plausible, with roughly a 1-2%

likelihood. Drought-Rain Volatility, reflecting years of extreme Rain Deficit followed or preceded by years of extreme rain excess (see Methods) becomes also twice as likely in the next 25 years, and by 2050-2075 could happen a third of the time.

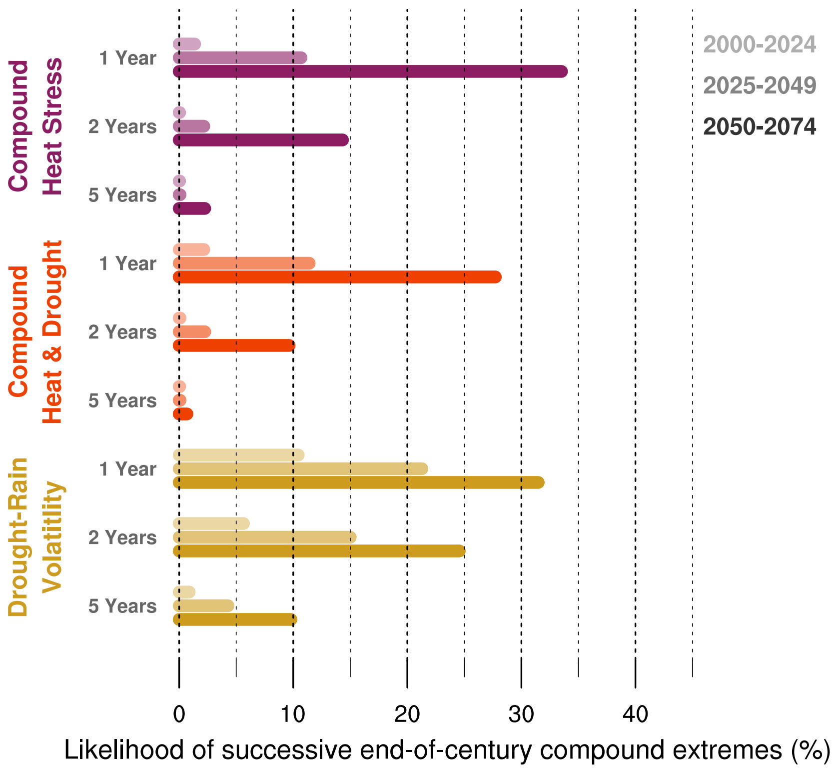

***Figure 3*: Likelihood of successive end-of-century compound extremes.** Likelihood of compound extremes occurring in one year, and that the following 2 or 5 years also exhibit compound extremes, for the periods starting in the years 2000-2024 (light colors), 2025-2049 (medium colors) and 2050-2075 (dark colors). Years of Compound Heat Stress are those extreme Excess Heat and extreme Night Heat and/or Humid Heat. Years of extreme Compound Heat and Drought are those exhibiting both extreme Excess Heat and Rain Deficit. Years of Drought-Rain Volatility are those exhibiting extreme Rain Deficit plus extreme Excess Rain the year before and/or the year after. Extreme years are defined as those equal or larger than the end-of-century 50th ensemble percentile averaged over the period of 2090-2099.

Distance to end-of-century decades and North Atlantic influence

Accumulated over 10-year periods, excess heat and drought stress varies widely from decade to decade under the same global warming levels, simply due to internal variability. Furthermore, the range of excess heat and drought stress that is possible in any given decade increases drastically under warming (Fig. 4). The decadal variability in these heat and drought excess metrics becomes so large that it can bring typical end-of-century conditions upon Europe already in the next few decades. Starting in 2040, 5-10% of the decades simulated by MPI-GE exceed end-of-century levels for all heat metrics, and this occurs already in 2020-

2029 for Rain Deficits. By 2060, the chances of heat and drought loaded decades that exceed typical-end-of-century levels rise to more than a 1 out of 10.

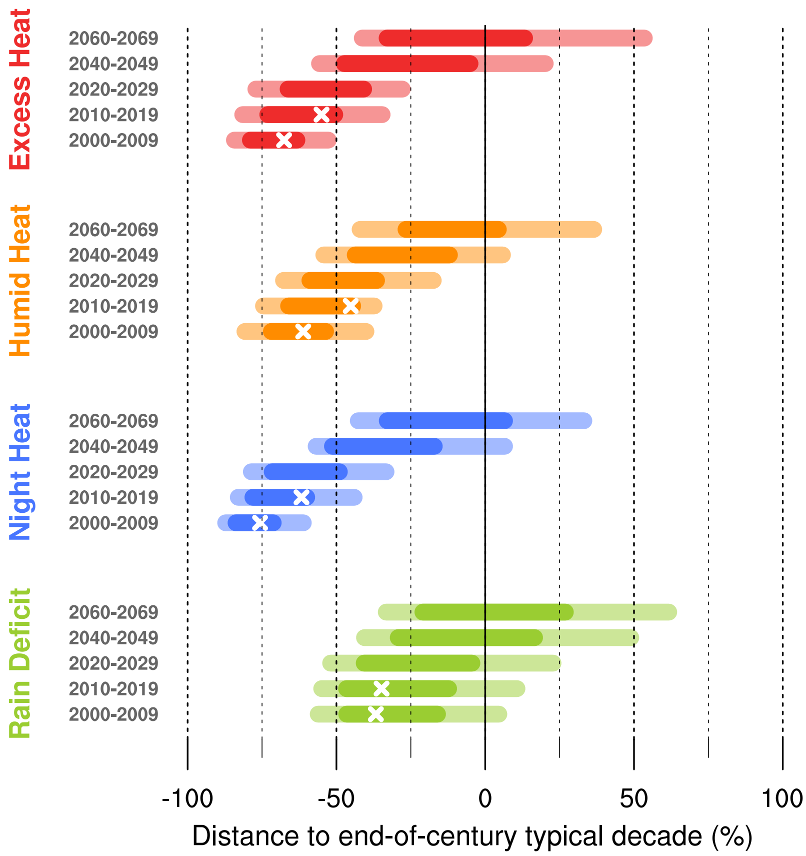

***Figure 4*: Distance to end-of-century decades.** Variability in excess metrics accumulated over a decade for the whole MPI-GE (pale colors) and for the range between the 10th to 90th percentiles of the ensemble distribution (bright colors), shown as distance to a typical end-of-century decade. White crosses mark observed decadal excess in E-OBS. Decadal excess metrics are calculated as the 10-year sum of the excess metrics. The distance to the end of the century average decade is calculated as the difference between each decadal excess metric minus the 50th ensemble percentile decadal excess in 2090-2099, divided by this 50th percentile and transformed to percentage. This difference is calculated against the ensemble 50th percentile both for each ensemble member and E-OBS.

This wide range of decadal excess heat and drought stress indicates that depending on the state of internal variability, some decades have stronger tendency toward successive extreme heat and drought stress than others. And these decadal differences are heavily dominated by the state of the North Atlantic climate system, as defined by its 10-year average SST-based AMV index (Methods). Positive AMV phases lead to an over 100% increase in the likelihood of exceeding typical end-of-century decadal heat stress already in the next decades (Fig. 5). The largest and most wide-spread increase in likelihood occurs for Humid Heat, followed by Night Heat. Thus, warm North Atlantic states increase the likelihood of concurrent heat and high humidity and night-time heat persistence, two of the forms of heat stress mostly linked to human heat-related morbidity. In contrast, the effect of AMV on Rain Deficit shows larger regional differences in MPI-GE, with typical end-of-century rain deficits being 25% more likely under positive AMV phases over Southern Europe and parts of Eastern Europe, but 10-25% more likely over parts of South-Eastern Europe under negative AMV.

A warm North Atlantic not only makes extreme decades for any given excess metric more likely, it also increases the likelihood of decades of compound end-of-century levels for two different forms of heat and drought stress occurring together (Fig. 6). During positive AMV phases, there is over a 1-in-10 chance of decades exceeding typical end-of-century levels already in 2030-2049 for compound day and nighttime Heat Excess, Humid and Night Heat and Heat and Drought. Heat and drought loaded decades exceeding end-of-century levels are twice as likely under positive versus negative AMV phases, and the most extreme decadal heat stress levels in all its forms occur always under warm North Atlantic states.

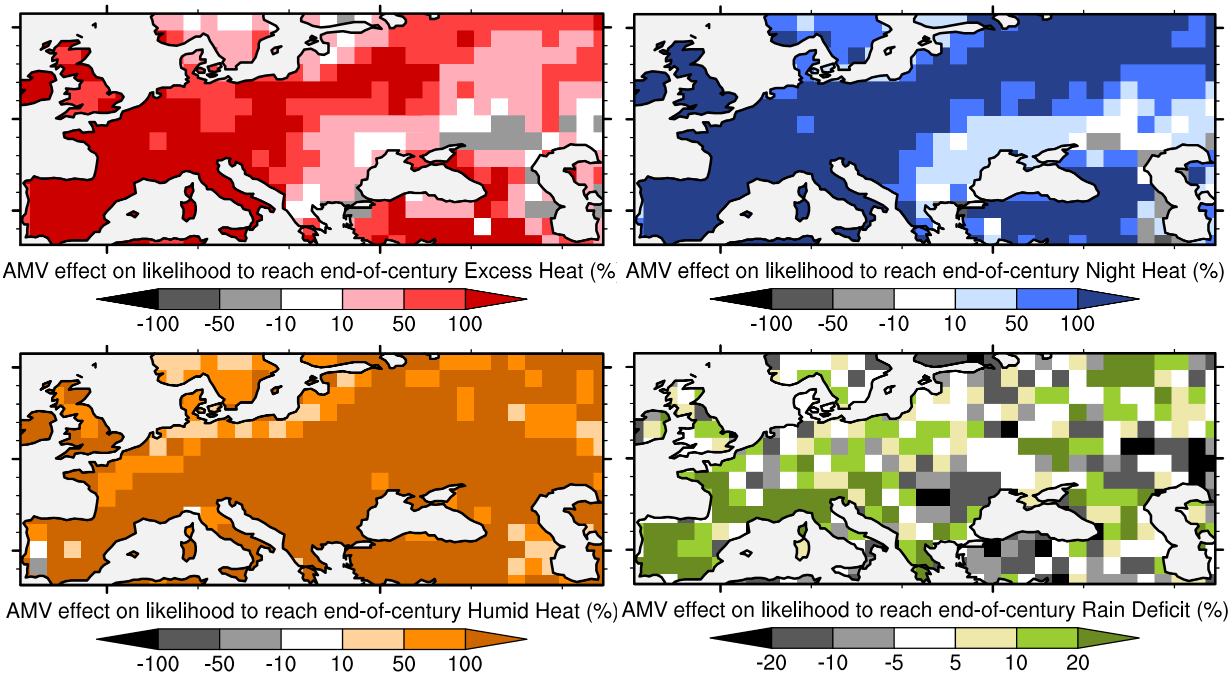

***Figure 5*: Effect of AMV phase on likelihood of reaching end-of-century levels.** Weighted difference in likelihood of decadal excess metrics starting in 2030-2049 reaching typical end-of-century levels under different concurrent AMV phases. Difference is shown as likelihood during AMV+ minus during AMV-, weighted by likelihood during AMV-, in percentage. Distance to typical end-of-century decades is the difference between each decadal excess metric at each grid cell, minus the ensemble mean decadal excess in 2090-2099, also at each grid cell. See SI Fig. S2 for non-weighted AMV-phase likelihoods and differences.

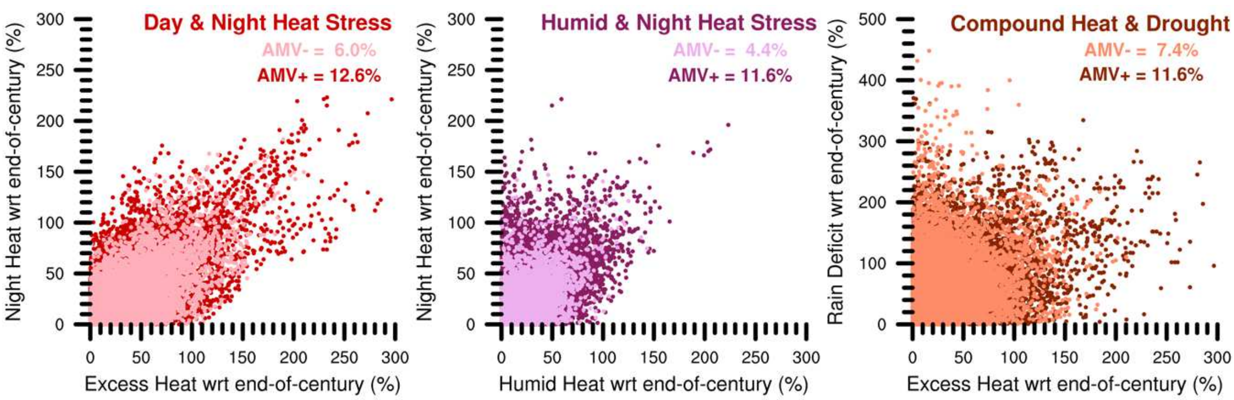

***Figure 6*: AMV effect on compound extremes.** Decades exceeding typical end-of-century levels in several heat and drought stress excess metrics under AMV+ (dark dots) and AMV- (light dots), starting in 2030-2049. Each dot represents one decade over one grid cell. Numbers indicate percentage of grid-cell decades that exceed end-of-century levels under each AMV phase. AMV is defined as the concurrent 10-year running mean of North Atlantic SSTs. Distance to end-of-century average calculated as the difference between each year values minus the decadal ensemble average over the period of 2090-2099, divided by the end-of-century average and transformed to percentage.

Discussion and Conclusions

We present the first assessment of how soon end-of-century heat and drought stress could occur over Europe in different forms, and the role that internal climate variability plays in producing the worst-case single, successive, and compounding end-of-century heat and drought. Our results are based on MPI-GE simulations, which are well in agreement with the variability and forced changes in observed excess temperature and precipitation. MPI-GE, the largest ensemble currently available, provides a precise sampling of low-probability events which is crucial for our analysis. This precise sampling of internal variability is key to robustly capture concurrent extreme conditions in more than one variable, or the conditional probabilities of experiencing extreme conditions again after an already extreme year. Furthermore, fully coupled Earth system model simulations that sufficiently capture the effect and variability of large-scale and long-term drivers, such as those of oceanic origin, are key to robustly assess the changing likelihood of such successive and compounding extremes.

To put these single-model results in context, with a moderate climate sensitivity of 2.8°C[45], MPI-GE is largely in agreement with multi-model projections for summer heat extremes, for which we have high confidence on both the sign and intensity of the projected changes[1]. In particular, across different climate models, MPI-ESM exhibits one of the lowest biases in reproducing observed temperature extremes[46], and projects changes in the characteristics of such extremes in line with other models[47]. On the other hand, for precipitation changes, MPI-GE shows one of the strongest summer precipitation decreases under warming over Central and Northern Europe[33]; and, among several other large ensembles, a comparatively strong increase in the frequency of consecutive drought years over Central Western Europe[34]. These findings are, however, only partially comparable to those presented here, due to our focus on not only summer but May-to-October for precipitation deficits, and a much larger region of study also including both Eastern and Southern Europe.

Our findings show that even under moderate warming, unprecedented levels of heat and drought stress typical of an end-of-century climate swiftly become a possibility over Europe in the near-term future. All heat stress forms considered are projected to reach or surpass end-of-century levels that were virtually impossible 20 years ago with a 1-in-10 likelihood as early as during the 2030-2039 decade. Moreover, succeeding extremes such end-of-century extreme single and compound heat and drought stress occurring repeatedly year after year, something that has not yet happened once in the observational record, becomes possible already in the next 30 years, with more than a 1-in-10 likelihood by 2050-2074. By then, two successive years of end-of-century rain-deficits are projected to occur 20% of the time, and there is a non-negligible chance of 5-year long continental scale mega-droughts.

Internal climate variability could bring any of these devastating occurrences typical of an end-of-the-century climate to Europe sooner than expected. This internal variability characterizes all the plausible summers that we could come to experience under the same global warming levels, and this range of plausible summers is growing wider by the decade. The range of potential heat and drought stress accumulated over a whole decade increases to the point that experiencing heat and drought loaded decades typical of an end-of-century climate could become a reality in Europe as early as 2040. This growing range of decadal variability in heat and drought stress over Europe is heavily influenced by the North Atlantic decadal variability. Our results show that under a concurrent warm North Atlantic state, exceeding end-of-century single and compound heat and drought stress during decades starting as early as in 2030 is twice as likely than under a cold North Atlantic state. This link between the comparatively highly predictable North Atlantic heat variability and such nearly impossible to predict multi-year periods of extreme heat and drought stress occurring well ahead of their time provides vital insights to increase our preparedness to some of the upcoming threats of climate change.

Methods

Observational and Model Data

Model simulations are fully-coupled, transient climate simulations from the Max Planck Institute Grand Ensemble[41] under historical and RCP4.5 forcing for the periods of 1950-2005 and 2006-2099, respectively. MPI-GE consists of 100 realizations of the same Earth System Model (MPI-ESM1.1), which is fairly similar to the CMIP6 version MPI-ESM1.2 and has a climate sensitivity of 2.8°C[45]. All of the 100 realizations use the same model physics and parametrizations and are driven by the same external forcings, but each start from a different initial climate state in 1850 taken from different points of the model's pre-industrial control run. MPI-ESM1.1 is used in the low-resolution (LR) configuration, with resolution T63 and 47 vertical levels in the atmosphere and 1.5° resolution and 40 vertical levels in the ocean.

Observational data from the E-OBS[48] dataset for the period of 1950-2021 are used for comparison and evaluation of the MPI-GE simulations against current climate conditions. E-OBS data, which has a native regular grid of 0.25 degree, are regridded to the coarser resolution of MPI-GE simulations. All spatial averages are calculated over land-only grid cells in the European area defined by the [35–63N, 10W–55E] latitude-longitude domain. When comparing against observations, model data are subsampled to grid boxes where observations are available.

Heat and Drought Stress Definitions

We use three heat stress indicators based respectively on summer (JJA) daily maximum temperatures, wet bulb temperatures reflecting the combined effect of heat and humidity, and daily minimum temperatures; and one meteorological drought metric based on May-to-October monthly precipitation. Wet bulb temperature is a multivariable metric calculated using daily average near-surface 2m air temperatures and relative humidity based on the method described in ref.[49]. Ideally, to obtain the most accurate wet bulb temperatures this should be calculated instantaneously at the model time step. However, this is not possible in MPI-GE, with currently only daily mean relative humidity output available. This approach can lead to a slight overestimation of absolute daily mean wet bulb temperatures based on instantaneous values[50], thus we base our analysis solely on relative changes and not on absolute values.

Excess Metrics for Heat and Drought

Based on these heat and drought stress indicators, we calculate excess metrics that capture extreme heat and drought occurring beyond certain thresholds, accumulated over the whole season. For heat-related excess metrics (i.e., Excess Heat, Humid Heat, and Night Heat) we calculate for each grid cell and day, the difference between the actual temperature reached (maximum daily temperature, wet bulb temperature, or minimum daily temperature for each metric, respectively) minus the given temperature threshold over said grid cell. Each heat excess metric is then calculated as the sum of this differences for all days above threshold per summer (JJA; as described in ref.[40]). The threshold is defined as the pooled daily 90th percentile level under historical conditions defined by the period of 1950-1999, to allow a comparison with E-OBS observations. Excess rain deficit is calculated similarly, but based on the difference between the monthly 10th percentile drought-threshold minus the actual monthly cumulative precipitation at each grid cell, for each month in the May-to-October period each year[32].

Compound excess metrics (i.e., Compound Heat Stress, Compound Heat and Drought, and Drought-Rain Volatility), are based on the same excess metrics co-occurring over their respective seasons, or following or preceding each other. Compound Heat Stress reflects Excess Heat and concurrent Humid Heat and/or Night Heat extreme conditions occurring together on any given year (JJA for heat metrics and May-October season for precipitation metrics). Compound Heat and Drought reflects simultaneous extreme Excess Heat and Rain Deficit conditions. Drought-Rain volatility reflects years of extreme Rain Deficits followed or preceded by years of extreme Rain Excess. Rain Excess is defined as the difference in monthly cumulative precipitation minus the 90th percentile in monthly precipitation for each month in the whole year.

Definition of extreme years and distance to end-of-century levels

We define extreme years in each excess metric as those years exceeding the typical end-of-century levels defined by the 50^{th} percentile of the ensemble spread, averaged over the period of 2090-2099. For the analysis in figures 2 and 3 we consider events with probabilities below 1% to be 'virtually impossible' and to have 'virtually zero' or 'negligible' likelihoods, while likelihoods above 1% are considered 'non-negligible' and thus events with likelihoods above 1% are here considered 'plausible'.

Typical end-of-century levels for decadal metrics, characterized by their start year, are defined as the 50th percentile of the ensemble distribution in 2090. Therefore, the distance to an end-of-century typical decade used in the analysis in Figs. 4, 5, and 6 is calculated as the difference between the decadal metric on any given start year minus this 50^{th} percentile in the decadal metric ensemble distribution in 2090. Additionally, for Fig. 4 we normalize this difference by the typical end-of-century value for each metric, thus dividing this difference by the 50^{th} percentile in the decadal metric ensemble distribution in 2090, and transform it to percentage. For assessments at the grid-cell level in Fig. 5 and 6, we substitute the 50^{th} percentile of the ensemble for the ensemble mean for computational efficiency, since both metrics yield comparable results.

Atlantic Multidecadal Variability Index definition

To capture the multi-year variability in North Atlantic temperatures, we use an AMV index defined as the 10-year mean SST in the region defined by the [20–60N, 70W–20W] latitude-longitude box. To remove forced effects we detrend each SST simulated time series by removing the ensemble mean at each grid cell[51], and normalize it by dividing it by its standard deviation. AMV phases are selected for start years when this AMV index is equal or larger to half standard deviation for positive phases, and equal or smaller than minus half standard deviation for negative phases.

Data availability

The MPI-GE simulations and model output are available for download at https://www.mpimet.mpg.de/en/grand-ensemble/ or by contacting grandensemble@mpimet.mpg.de. E-OBS observational data are available for download at https://www.ecad.eu/download/ensembles/download.php

Code availability

The scripts used to perform this analysis and other supporting information that may be useful in reproducing this work are archived by the Library and Information Service at the Max Planck Institute for Meteorology and are freely available by contacting publications@mpimet.mpg.de. The analysis and figures in this article were performed using Climate Data Operator (CDO) software (Schulzweida, 2022) the NCAR Command Language (NCAR 2019; Version 6.6.2).

References

1. Seneviratne, S.I., X. Zhang, M. Adnan, W. Badi, C. Dereczynski, A. Di Luca, S. Ghosh, I. Iskandar, J. Kossin, S. Lewis, F. Otto, I. Pinto, M. Satoh, S.M. Vicente-Serrano, M. Wehner, and B. Zhou, 2021: Weather and Climate Extreme Events in a Changing Climate. In Climate Change 2021: The Physical Science Basis. Contribution of Working Group I to the Sixth Assessment Report of the Intergovernmental Panel on Climate Change [Masson- Delmotte, V., P. Zhai, A. Pirani, S.L. Connors, C. Péan, S. Berger, N. Caud, Y. Chen, L. Goldfarb, M.I. Gomis, M. Huang, K. Leitzell, E. Lonnoy, J.B.R. Matthews, T.K. Maycock, T. Waterfield, O. Yelekçi, R. Yu, and B. Zhou (eds.)]. Cambridge University Press, Cambridge, United Kingdom and New York, NY, USA, pp. 1513–1766, doi:10.1017/9781009157896.013.

2. Suarez-Gutierrez L., Li C., Müller W. A., Marotzke J. (2018). Internal variability in European summer temperatures at 1.5C and 2C of global warming. Environ. Res. Lett. 13 064026. https://doi.org/10.1088/1748-9326/aaba58

3. Barriopedro, B., E. M. Fischer, J. Luterbacher, R. M. Trigo, R. G.-Herrera, The hot summer of 2010: Redrawing the temperature record map of Europe. Science 332, 220–224 (2011).

4. Fischer, E.M., Sippel, S. & Knutti, R. Increasing probability of record-shattering climate extremes. Nat. Clim. Chang. 11, 689–695 (2021). https://doi.org/10.1038/s41558-021-01092-9

5. Watts N, Amann M, Arnell N, Ayeb-Karlsson S, Beagley J, Belesova K, Boykoff M, Byass P, Cai W, Campbell-Lendrum D, Capstick S, Chambers J, Coleman S, Dalin C, Daly M, Dasandi N, Dasgupta S, Davies M, Di Napoli C, Dominguez-Salas P, Drummond P, Dubrow R, Ebi KL, Eckelman M, Ekins P, Escobar LE, Georgeson L, Golder S, Grace D, Graham H, Haggar P, Hamilton I, Hartinger S, Hess J, Hsu SC, Hughes N, Jankin Mikhaylov S, Jimenez MP, Kelman I, Kennard H, Kiesewetter G, Kinney PL, Kjellstrom T, Kniveton D, Lampard P, Lemke B, Liu Y, Liu Z, Lott M, Lowe R, Martinez-Urtaza J, Maslin M, McAllister L, McGushin A, McMichael C, Milner J, Moradi-Lakeh M, Morrissey K, Munzert S, Murray KA, Neville T, Nilsson M, Sewe MO, Oreszczyn T, Otto M, Owfi F, Pearman O, Pencheon D, Quinn R, Rabbaniha M,

Robinson E, Rocklöv J, Romanello M, Semenza JC, Sherman J, Shi L, Springmann M, Tabatabaei M, Taylor J, Triñanes J, Shumake-Guillemot J, Vu B, Wilkinson P, Winning M, Gong P, Montgomery H, Costello A. (2021). The 2020 report of The Lancet Countdown on health and climate change: responding to converging crises. Lancet. 9;397 (10269):129-170, https://doi.org/10.1016/s0140-6736(20)32290-x

6. Vicedo-Cabrera, A. M., N. Scovronick, F. Sera, D. Royé, R. Schneider, A. Tobias, C. Astrom, Y. Guo, Y. Honda, D. M. Hondula, R. Abrutzky, S. Tong, M. de Sousa Zanotti Stagliorio Coelho, P. H. Nascimento Saldiva, E. Lavigne, P. Matus Correa, N. Valdes Ortega, H. Kan, S. Osorio, J. Kyselý, A. Urban, H. Orru, E. Indermitte, J. J. K. Jaakkola, N. Ryti, M. Pascal, A. Schneider, K. Katsouyanni, E. Samoli, F. Mayvaneh, A. Entezari, P. Goodman, A. Zeka, P. Michelozzi, F. de'Donato, M. Hashizume, B. Alahmad, M. Hurtado Diaz, C. De La Cruz Valencia, A. Overcenco, D. Houthuijs, C. Ameling, S. Rao, F. Di Ruscio, G. Carrasco-Escobar, X. Seposo, S. Silva, J. Madureira, I. H. Holobaca, S. Fratianni, F. Acquaotta, H. Kim, W. Lee, C. Iniguez, B. Forsberg, M. S. Ragettli, Y. L. L. Guo, B. Y. Chen, S. Li, B. Armstrong, A. Aleman, A. Zanobetti, J. Schwartz, T. N. Dang, D. V. Dung, N. Gillett, A. Haines, M. Mengel, V. Huber, A. Gasparrini (2021). The burden of heat-related mortality attributable to recent human-induced climate change. Nat. Clim. Chang. 11, 492–500, https://doi.org/10.1038/s41558-021-01058-x

7. Orlov, A., Sillmann, J., Aunan, K., Kjellstrom, T., & Aaheim, A. (2020). Economic costs of heat-induced reductions in worker productivity due to global warming. Global Environmental Change, 63, 102087. https://doi.org/10.1016/j.gloenvcha.2020.102087

8. García-León, D., Casanueva, A., Standardi, G. et al., Current and projected regional economic impacts of heatwaves in Europe. Nat Commun 12, 5807 (2021). https://doi.org/10.1038/s41467-021-26050-z

9. Ruffault, J., Curt, T., Moron, V. et al., Increased likelihood of heat-induced large wildfires in the Mediterranean Basin. Sci Rep 10, 13790 (2020). https://doi.org/10.1038/s41598-020-70069-z

10. Brás, T. A., Seixas, J., Carvalhais, N., & Jägermeyr, J. (2021). Severity of drought and heatwave crop losses tripled over the last five decades in Europe. Environmental Research Letters, 16. https://doi.org/10.1088/1748-9326/abf004

11. Sherwood, S.C., Huber, M. (2010). An adaptability limit to climate change due to heat stress. Proc Natl Acad Sci 107(21):9552–9555. https://doi.org/10.1073/pnas.0913352107

12. Zscheischler, J., Martius, O., Westra, S., Bevacqua, E. R. C., Horton, R. M., van den Hurk, B., AghaKouchak, A., Jézéquel, A., Mahecha, M. D., Maraun, D., Ramos, A. M., Ridder, N., Thiery, W., and Vignotto, E. (2020). A typology of compound weather and climate events, Nat. Rev. Earth Environ., 1, 333–347, https://doi.org/10.1038/s43017-020-0060-z

13. Royé D., F. Sera, A. Tobías, R. Lowe, A. Gasparrini, M. Pascal, F. de'Donato, B. Nunes and J. P. Teixeira, (2021). Effects of Hot Nights on Mortality in Southern Europe, Epidemiology, Volume 32, Issue 4, p 487-498, https://doi.org/10.1097/ede.0000000000001359

14. Feller, U., Kingston-Smith, A. H., Centritto, M. (2017). Editorial: abiotic stresses in agroecology: a challenge for whole plant physiology. Front Environ Sci 5:13. https://doi.org/10.3389/fenvs.2017.00013

15. Wehner M., Stone D., Krishnan H., AchutaRao K., Castillo F. (2016). The deadly combination of heat and humidity in India and Pakistan in summer 2015. Bull. Am. Meteorol. Soc. 97(12):S81–S86. https://doi.org/10.1175/BAMS-D-16-0145.1

16. Robine, J.M., Cheung, S.L.K., Roy, S.L., Oyen, H.V., Griffiths, C., Michel, J.P., Herrmann. F.R. (2008) Death toll exceeded 70,000 in europe during the summer of 2003. CR Biol 331(2):171–178. https://doi.org/10.1016/j.crvi.2007.12.001

17. Schuldt, B., Buras, A., Arend, M., Vitasse, Y., Beierkuhnlein, C., Damm, A., Gharun, M., Grams, T. E. E., Hauck, M., Hajek, P., Hartmann, H., Hiltbrunner, E., Hoch, G., Holloway-Phillips, M., Körner, C., Larysch, E., Lübbe, T., Nelson, D. B., Rammig, A., Rigling, A., Rose, L., Ruehr, N. K., Schumann, K., Weiser, F., Werner, C., Wohlgemuth, T., Zang, C. S., and Kahmen, A. (2020). A first assessment of the impact of the extreme 2018 summer drought on Central European forests, Basic Appl. Ecol., 45, 86–103, https://doi.org/10.1016/j.baae.2020.04.003

18. Toreti, A., Belward, A., Perez-Dominguez, I., Naumann, G., Luterbacher, J., Cronie, O., et al., (2019). The exceptional 2018 European water seesaw calls for action on adaptation. Earth's Future, 7, 652– 663. https://doi.org/10.1029/2019EF001170

19. AghaKouchak, A., Chiang, F., Huning, L. S., Love, C. A., Mallakpour, I., Mazdiyasni, O., Moftakhari, H., Papalexiou, S. M., Ragno, E., and Sadegh, M., Climate extremes and compound hazards in a warming world. Annu. Rev. Earth Planet. Sci. 48, 519–548 (2020). https://doi.org/10.1146/annurev-earth-071719-055228

20. de Ruiter, M. C., Couasnon, A., van den Homberg, M. J. C., Daniell, J. E., Gill, J. C., & Ward, P. J. (2020). Why we can no longer ignore consecutive disasters. Earth's Future, 8, e2019EF001425. https://doi.org/10.1029/2019EF001425

21. Bastos, A., Orth, R., Reichstein, M., Ciais, P., Viovy, N., Zaehle, S., Anthoni, P., Arneth, A., Gentine, P., Joetzjer, E., Lienert, S., Loughran, T., McGuire, P. C., O, S., Pongratz, J., and Sitch, S. (2021) Vulnerability of European ecosystems to two compound dry and hot summers in 2018 and 2019, Earth Syst. Dynam., 12, 1015–1035, https://doi.org/10.5194/esd-12-1015-2021

22. Callahan, C. W., and Mankin, J. S. (2022). Globally unequal effect of extreme heat on economic growth. Sci. Ad., Vol 8, Issue 43, DOI: 10.1126/sciadv.add3726

23. Sutton, R. T., and D. L. Hodson (2005) Ocean science: Atlantic Ocean forcing of North American and European summer climate. Science, 309, 115–118, https://doi.org/10.1126/science.1109496.

24. Sutton, R., Dong, B. Atlantic Ocean influence on a shift in European climate in the 1990s. Nature Geosci 5, 788–792 (2012). https://doi.org/10.1038/ngeo1595

25. Ghosh, R., W. A. Müller, J. Baehr, and J. Bader (2017). Impact of observed North Atlantic multi-decadal variations to European summer climate: a linear baroclinic response to surface heat-ing. Clim. Dyn. 48:3547. 10.1007/s00382-016-3283-4

26. Lesk, C. and Anderson, W. (2021). Decadal variability modulates trends in concurrent heat and drought over global croplands Environ. Res. Lett. 16 055024. https://doi.org/10.1088/1748-9326/abeb35

27. Qasmi, S., Sanchez-Gomez, E., Ruprich-Robert, Y., Boé, J., & Cassou, C. (2021). Modulation of the Occurrence of Heatwaves over the Euro-Mediterranean Region by the Intensity of the Atlantic Multidecadal Variability, Journal of Climate, 34(3), 1099-1114. https://doi.org/10.1175/JCLI-D-19-0982.1

28. Hodson, D.L.R., Bretonnière, PA., Cassou, C. et al., Coupled climate response to Atlantic Multidecadal Variability in a multi-model multi-resolution ensemble. Clim Dyn 59, 805–836 (2022). https://doi.org/10.1007/s00382-022-06157-9

29. Hellmich, L., D. Matei, L. Suarez-Gutierrez, W. A. Müller (Under Review in npj Climate and Atmospheric Science). Extremely Warm European Summers driven by North Atlantic Heat Inertia.

30. Samaniego, L., Thober, S., Kumar, R. et al., Anthropogenic warming exacerbates European soil moisture droughts. Nature Clim Change 8, 421–426 (2018). https://doi.org/10.1038/s41558-018-0138-5

31. Suarez-Gutierrez L., Li C., Müller W. A., Marotzke J. (2020). Dynamical and thermodynamical drivers of variability in European summer heat extremes. Clim. Dyn. 54:4351–4366, https://doi.org/10.1007/s00382-020-05233-2

32. Raymond, C., L. Suarez-Gutierrez, K. Kornhuber, M. A. Pascolini-Campbell, J. Sillmann, D. E. Waliser (2022) Increasing spatiotemporal proximity of heat and precipitation extremes in a warming world quantified by a large model ensemble. Environ. Res. Lett. 17 035005. https://doi.org/10.1088/1748-9326/ac5712

33. Bevacqua, E., Zappa, G., Lehner, F., Zscheischler, J. Precipitation trends determine future occurrences of compound hot–dry events. Nat. Clim. Chang. (2022). https://doi.org/10.1038/s41558-022-01309-5

34. van der Wiel, K., Batelaan, T.J. & Wanders, N. (2022) Large increases of multi-year droughts in north-western Europe in a warmer climate. Clim Dyn (2022). https://doi.org/10.1007/s00382-022-06373-3

35. Gao, M., Yang, J., Gong, D., Shi, P., Han, Z., & Kim, S. (2019). Footprints of Atlantic Multidecadal Oscillation in the Low-Frequency Variation of Extreme High Temperature in the Northern Hemisphere, Journal of Climate, 32(3), 791-802. https://doi.org/10.1175/JCLI-D-18-0446.1

36. Borchert, L., H. Pohlmann, J. Baehr, N.-C. Neddermann, L. Suarez-Gutierrez, W. A. Müller (2019). Decadal predictions of the probability of occurrence for warm summer temperature extremes. Geophysical Research Letters, 16, 14042-14051. doi:10.1029/2019GL085385

37. Müller, W. A., Borchert, L., & Ghosh, R. (2020). Observed subdecadal variations of European summer temperatures. Geophysical Research Letters, 47, e2019GL086043. https://doi.org/10.1029/2019GL086043

38. Ghosh, R., Müller, W.A., Eichhorn, A., Baher, J., Bader, J. (2019) Atmospheric pathway between Atlantic multidecadal variability and European summer temperature in the atmospheric general circulation model ECHAM6. Clim Dyn 53, 209–224. https://doi.org/10.1007/s00382-018-4578-4

39. Yeager, S.G., Robson, J.I. (2017) Recent Progress in Understanding and Predicting Atlantic Decadal Climate Variability. Curr Clim Change Rep 3, 112–127. https://doi-org.e-bis.mpimet.mpg.de/10.1007/s40641-017-0064-z

40. Perkins-Kirkpatrick, S.E., Lewis, S.C. Increasing trends in regional heatwaves. Nat Commun 11, 3357 (2020). https://doi.org/10.1038/s41467-020-16970-7

41. Maher, N., Milinski, S., Suarez-Gutierrez, L., Botzet, M., Dobrynin, M., Kornblueh, L., Kröger, J., Takano, Y., Ghosh, R., Hedemann, C., Li, C., Li, H., Manzini, E., Notz, D., Putrasahan, D., Boysen, L., Claussen, M., Ilyina, T., Olonscheck, D., Raddatz, T., Stevens, B., Marotzke, J. (2019) The Max Planck Institute Grand Ensemble: enabling the exploration of climate system variability. JAMES 11(7):2050–2069. https://doi.org/10.1029/2019MS001639

42. Bevacqua, E., Suarez-Gutierrez, L., Jézéquel, A., Lehner, F., Vrac, M., Yiou, P., Zscheischler, J. (Under Review in Nature Communications). Advancing our understanding of compound weather and climate events via large ensemble model simulations

43. Suarez-Gutierrez, L., Milinski, S., Maher, N. Exploiting large ensembles for a better yet simpler climate model evaluation. Clim Dyn 57, 2557–2580 (2021). https://doi.org/10.1007/s00382-021-05821-w

44. Wood, R. R., Lehner, F., Pendergrass, A. G., and Schlunegger, S. (2021) Changes in precipitation variability across time scales in multiple global climate model large ensembles. Environ. Res. Lett. 16 084022

45. Mauritsen, T., Bader, J., Becker, T., Behrens, J., Bittner, M., Brokopf, R., et al., (2019). Developments in the MPI-M Earth System Model version 1.2 (MPI-ESM1.2) and its response to increasing CO2. Journal of Advances in Modeling Earth Systems, 11, 998–1038. https://doi.org/10.1029/2018MS001400

46. Di Luca, A., Pitman, A. J., & de Elía, R. (2020). Decomposing temperature extremes errors in CMIP5 and CMIP6 models. Geophysical Research Letters, 47, e2020GL088031. https://doi.org/10.1029/2020GL088031

47. Schoetter, R., Cattiaux, J. & Douville, H. (2015) Changes of western European heat wave characteristics projected by the CMIP5 ensemble. Clim Dyn 45, 1601–1616.

48. Cornes, R. C., van der Schrier, G., van den Besselaar, E. J. M., & Jones, P. D. (2018). An ensemble version of the E-OBS temperature and precipitation data sets. Journal of Geophysical Research: Atmospheres, 123, 9391– 9409. https://doi.org/10.1029/2017JD028200

49. Stull R (2011) Wet-bulb temperature from relative humidity and air temperature. J Appl Meteorol Climatol 50(11):2267–2269. https://doi.org/10.1175/JAMC-D-11-0143.1

50. Buzan, J. R., Oleson, K., and Huber, M.: Implementation and comparison of a suite of heat stress metrics within the Community Land Model version 4.5, Geosci. Model Dev., 8, 151–170, https://doi.org/10.5194/gmd-8-151-2015, 2015.

51. Deser, C., & Phillips, A. S. (2021). Defining the internal component of Atlantic Multidecadal Variability in a changing climate. Geophysical Research Letters, 48, e2021GL095023. https://doi. org/10.1029/2021GL095023

52. Schulzweida, Uwe. (2022). CDO User Guide (2.1.0). Zenodo. https://doi.org/10.5281/zenodo.7112925

Acknowledgements

This project was supported by the Max Planck Society for the Advancement of Science and by the German Ministry of Education and Research (BMBF) under the ClimXtreme project, subproject DecHeat (Grant number 01LP1901F). LSG has also received funding from the European Union's Horizon Europe Framework Programme under the Marie Skłodowska-Curie grant agreement No 101064940. We thank Leonard Borchert for providing insightful comments and suggestions to improve this work. We acknowledge Sebastian Brune and Johanna Baehr for producing and processing the historical and RCP4.5 MPI Grand Ensemble simulations used in this study, and the Swiss National Computing Centre (CSCS) and the German Climate Computing Center (DKRZ) for providing the necessary computational resources. This work used resources of the Deutsches Klimarechenzentrum (DKRZ) granted by its Scientific Steering Committee (WLA) under project ID bb1152.

Author Contributions

LSG designed and performed the analysis and drafted the manuscript, WM and JM contributed to shaping the research and to the interpretation of the results, and provided feedback on the manuscript.

Supplementary Information

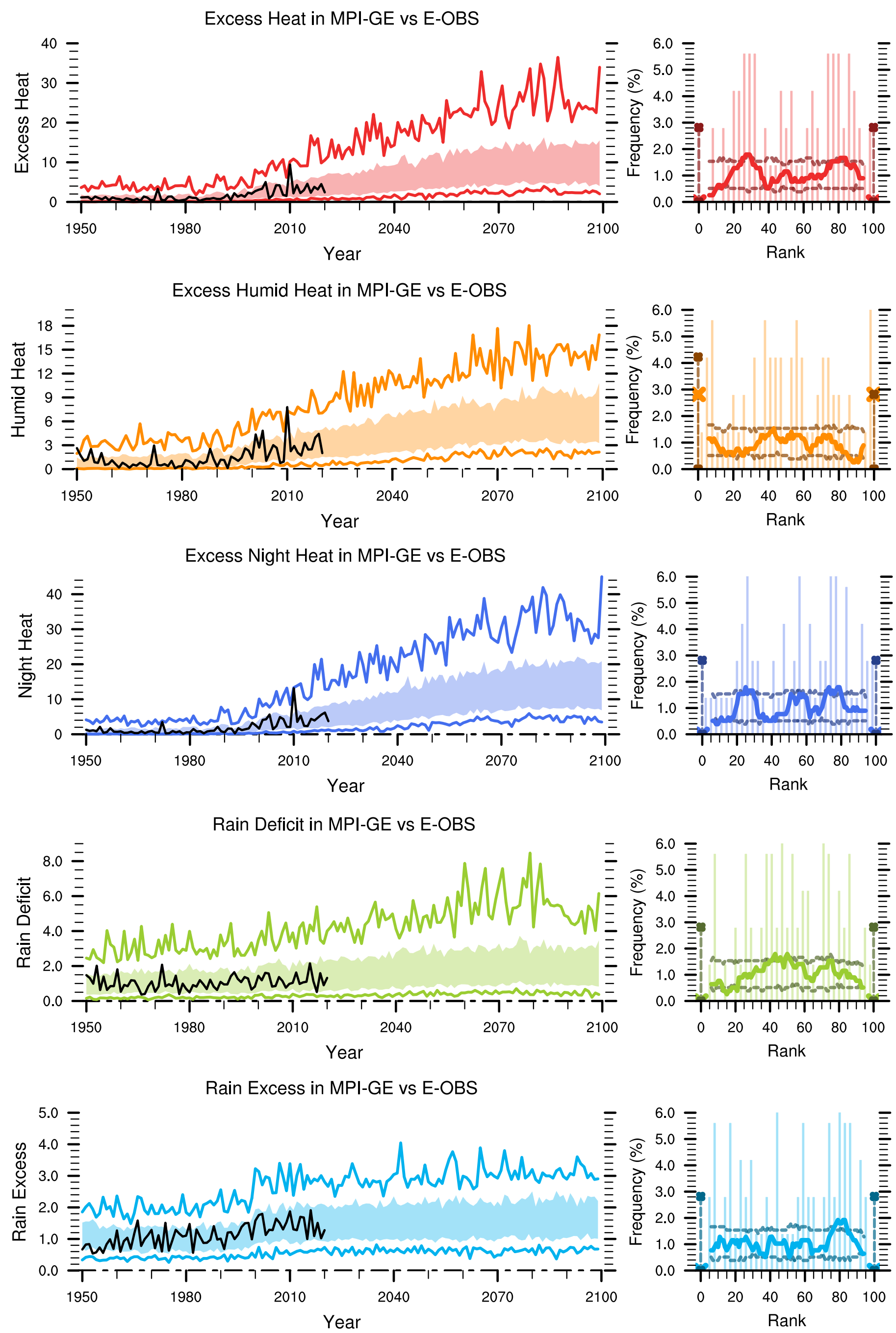

Figure S1: **Evaluation of excess metrics by MPI-GE vs. E-OBS observations.** Time series (left) and rank histograms (right) for MPI-GE simulations (color) and E-OBS observations (black; 1950-2021). Color lines show ensemble maxima and minima, shading shows the ensemble spread within the 10th-90th percentile bounds. Metrics are shown as ratios with respect to their 1950-1999 average. Rank histograms represent the frequency of each place that E-OBS values would take in a list of ensemble members ordered by ascending values. Lines illustrate the mean rank frequency over a centered 10-bin window for E-OBS (solid bright lines), and for the 90% confidence perfect model range (5th-95th percentiles) of rank slopes for each ensemble member treated as observations (dashed dark lines). Crosses show the frequency of minimum (0) and maximum (100, number of members) ranks for E-OBS (bright colors), and the perfect model 5th-95th percentile range in frequency (dark colors). Bin size for ranks 1 to 99 is 6 to aid visualization. See Suarez-Gutierrez et al., 2021 for details on this evaluation framework.

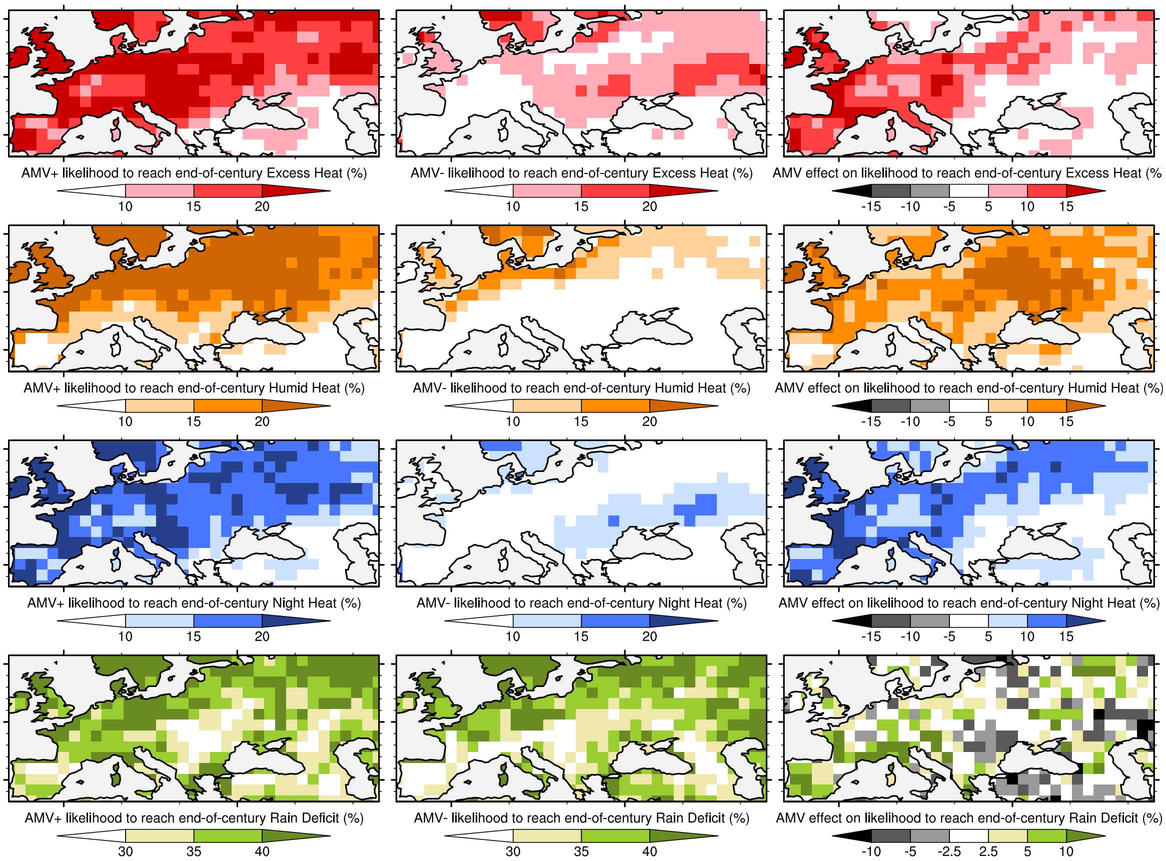

***Figure S2*: Effect of AMV phase on likelihood of reaching end-of-century levels.** Likelihood of decadal excess metrics with start years in the period of 2030-2049 reaching end-of-century average decadal levels under different AMV phases, and their difference (AMV+ minus AMV-). The distance to the end of the century average decade is calculated as the difference between each decadal excess metric anomaly at each grid cell, minus the ensemble mean decadal excess in 2090-2099, also at each grid cell.